International Journal of ChemTech Research
CODEN(USA): IJCRGG ISSN : 0974-4290
Vol.4, No.4, pp 1686-1700, Oct-Dec 2012

Characterization And Adsorption Studies Of "Lagenaria siceraria" Shell Carbon For The Removal Of Fluoride

Y.Hanumantharao[1]*, Medikondu Kishore[2], K.Ravindhranath[3]

[1]Andhra Loyola College (Autonomous), Vijayawada, Krishna Dist., Andhra Pradesh, India-520008,

[2]Department of Chemistry, PSCMR College of Engineering and Technology, Vijayawada, Krishna Dist., Andhra Pradesh, India-520001,

[3]Department of Chemistry, Bapatla Engineering College, Bapatla, Guntur Dist., Andhra Pradesh, India-522101.

Corres. Author : yhr.chaya@yahoo.com

Abstract: The surface sorption characteristics of activated carbon prepared from the shells of "Lagenaria siceraria" (calabash or bottle gourd or opo squash or long melon) towards fluoride has been investigated by varying the operational parameters such as initial concentrations, (1.5-15 mg/L), agitation time (10-70 minutes) and pH (3-10). Batch processes are employed. The experimental isotherms data are analyzed using Langmuir and Freundlich isotherm models. The data is best fitted with the Langmuir isotherm model. The calculated dimensionless separation factor, R_L indicates that the adsorption of F^- ion onto adsorbent is favorable. First order, pseudo-first order, second order and pseudo-second order kinetic equations and intra particle diffusion and pore diffusion models are used to examine the experimental data. It is found that the pseudo-second order kinetic equation describes the data of F^- ion adsorption on adsorbent carbon adequately. The BET surface area pore size distributions, and physicochemical parameters for the adsorbent are obtained by N_2 adsorption at 77 K. Surface morphology is also examined using Scanning Electron Microscopy (SEM), Energy Dispersive Spectroscopy (EDX) and X-ray Photo Electron Spectroscopy (XPS) before and after adsorption of F^- ion. The chemical composition, elemental analysis and functional groups on the surface of the active carbon prepared are studied using XRD, and FT-IR techniques.
Key words: Lagenaria siceraria, Activated carbon, fluoride ion, adsorption, characterization, kinetic study and isotherms.

Introduction

Fluoride has a significant mitigating effect on human health and its continuing consumption of higher concentrations cause dental fluorosis and in extreme cases even skeletal fluorosis[1]. It is supposed to be more toxic than lead[2]. Fluoride pollution is due to natural and anthropogenic sources[3] and its maximum permissible limit in drinking water as per WHO guidelines is: 1.5 mg/L[4]

Researchers are trying to evolve methodologies for controlling this potential health hazard. Several procedures have been developed, both in field and lab, based on precipitation[5- 7], membrane processes[8], electrochemical decomposition[9], ion-exchange [10] and sorption properties of adsorbents [11]

Zirconium impregnated coconut shell carbon[12], nitric acid treated Mango shell carbon[13-15] and Sulphonated coconut shell carbon[16], have also been studied in controlling the fluoride pollution. The sorption abilities of carbons of Cashew nut shell[16], ground nut shell[17], Acasia Fernisiana[18] and Palmyra male influroresence[19] and Acacia Arabica dry fruit[1],are explored for their sorption abilities in the removal of Fluoride from waters.

The use of activated Carbons derived from bio-waste materials is found to be promising alternative than the traditional and conventional methods in controlling the pollution problems. Active carbons of Coconut coir pith[20], water hyacinth[21], Neem leafs (Azadirakta indica), papal leaves (Ficus religiosa), khair leafs (Acacia catechu wild) [2], Emblica phyllanthus [22] and Morringa[23] have been investigated for their sorption ability for fluoride ions.

These methods though have achieved some degree of success, universally acceptable simple, effective and economical method, is still eluding the researchers.

In this contest the methods based on active carbons are found to be interesting owing to the fact that these substances are endowed with large surface area, micropore structure, high adsorption capacity and high degree of surface reactivity. Further, the carbon atoms located at the surface and edges of carbon crystallites in the sorbent, act as active sites and are showing a strong tendency to chemisorb adsorbates and give rise to non-stoichiometric stable surface compounds called surface complexes. Among these surface complexes, surface oxygen complexes are reported to be responsible for many physicochemical and surface properties [24] and efforts have also been directed towards elucidating the surface chemistry of such materials[25]. With the availability of modern sophisticated techniques like XPS, FTIR SEM-EDX, a thorough understanding of surface chemistry of active carbons with respect to the nature of surface groups, their interaction with absorbate molecules and type of bonding, is possible and these techniques are proving to be complementary to the quantitative chemical methods of assessment[25-26].

In the present work, active carbon derived from 'Lagenaria siceraria' shell (LSSC) has been explored for its sorption properties towards fluoride, its effectiveness in removing the fluoride ions from aqueous solutions at low concentrations and further, its sorption nature has been characterized and effectively accounted by the kinetic , isothermal and surface morphological studies.

Materials And Experimental Procedures

Reagents and chemicals

All reagents and chemicals used in the present investigation were of AR grade purchased from Ranbaxy Co. Pvt. Ltd. India and all solutions were prepared by using fluoride free double distilled water.

Adsorbent materials

Lagenaria siceraria (Fig.1), long melon (English), belongs to Cucurbitaceae family in plant kingdom and is well grown in many parts of the world. This can either be harvested as young and is used as a vegetable, or harvested until matured, dried, and then it is used as a bottle, utensil, or pipe. Hence the name bottle gourd.

Fig. 1: Lagenaria siceraria fruit with stem and dried fruit

Adsorbent carbon preparation

Lagenaria siceraria dry shells were collected in bulk, crushed and washed in cold water to remove dust. Then they were dried in sunlight about one week and cut into small pieces and carbonized in muffle furnace (in absence of air) for about 7 hours at 700^{o}C. After carbonization, carbon was poured in fluoride free water (double distilled water), filtered and washed several times with cold fluoride free water and dried in an air oven at 110^{o}C for overnight. Then, the carbon was sieved into desired particle sizes. The carbonized material (LSSC) in powder form (about 50 g) was taken in one liter volumetric flask and mixed with approximately 800 ml of 0.1M solution HNO_3 and boiled for 2 to 3 hours on flame for Liquid phase oxidation. After acid treatment, they were filtered and washed several times with hot water to remove un-reacted acid from carbon surface, until the effluent pH: 7 was retained.

Defluoridation: 100 ml of standard fluoride solution (5 mg/L) was pipette out into a 500 ml beaker. To it, 0.5g/L of the prepared carbon was added and stirred at 200 rpm mechanically for 30 minutes. Then, the solution was filtered through Whatman No- 42 filter paper. The F^- ion concentration in the sample after defluoridation was determined using ion-selective electrode specific to fluorides. The same procedure was adopted for the experiments carried out by varying other parameters.

Surface characterization of activated carbons-FTIR analysis: The adsorbents were examined using Fourier Transform Infrared spectroscopy (FTIR). The sample discs were prepared by mixing of 1 mg of powdered carbon with 500 mg of KBr (Merck; for spectroscopy) in an agate mortar, then pressing the resulting mixture successively under a pressure of 5 tones/ cm^2 for about 5 min., and at 10 tones/cm^2 for 5 min., under vacuum. Then, the spectra were measured from 4000 to 400 cm^{-1} on a JASCO-FTIR-5300 model.

X- Ray Photoelectron Spectroscopy (XPS): The prepared activated carbon samples were analyzed on KRATOS AXIS 165 under 10^{-9} torr vacuum with dual Al-Mg-anodes using Mg K radiation. Pass energy of 80 eV was used in recording the spectra. X-ray excitation source was Mg K (1253.06 eV) and hemi spherical electron analyzer was used. The samples were dried at 283 k for 24 h before the analysis. Survey and high resolution narrow scans were recorded for C 1s, O 1s, and F 1s photoelectron peaks. The atomic concentrations were calculated from the photoelectron peak areas using Shirley background subtraction and sensitivity factors were taken from PHI. The obtained XPS spectra were fitted using a non linear square method with the convolution of Lorentzian and Gaussian functions after the polynomial background subtraction from the raw data.

Scanning electron microscope-Energy dispersive x-ray spectroscopy (SEM-EDAX): The surfaces of the powder of carbonaceous materials were stubbed using the double-sided adhesive carbon tape. Samples were coated with a thin layer of platinum with the help of platinum coater (JOEL Auto fine coater model, JFC –1600 auto fine coater; Coating time : 120 sec with 20mA). The microphotographs of these samples were recorded using SEM JEOL model: JSM-5600 which was equipped with EDX Analyzer with an accelerating voltage of 5 kV, at high vacuum mode. The maximum magnification possible in the equipment was 3,00,000 times with a resolution of 3 nm and it could be typically setting at various magnifications for all the samples of study.

BET-Surface area: BET theory aims to explain the physical adsorption of gas molecules on a solid surface and serves as the basis for an important analysis technique for the measurement of the specific surface area of a material. BET-N_2 adsorption experiments were carried out manometrically using Quanta chrome Nova Win - Data Acquisition and Reduction for NOVA instruments version 10.01. All samples were degassed overnight at 200^{o}C, prior to the adsorption experiments. The BET-N_2 surface area was obtained by applying the BET equation to the adsorption data. The pore volume and pore size of the active carbon, LSSC, were determined by applying t-method.[27]

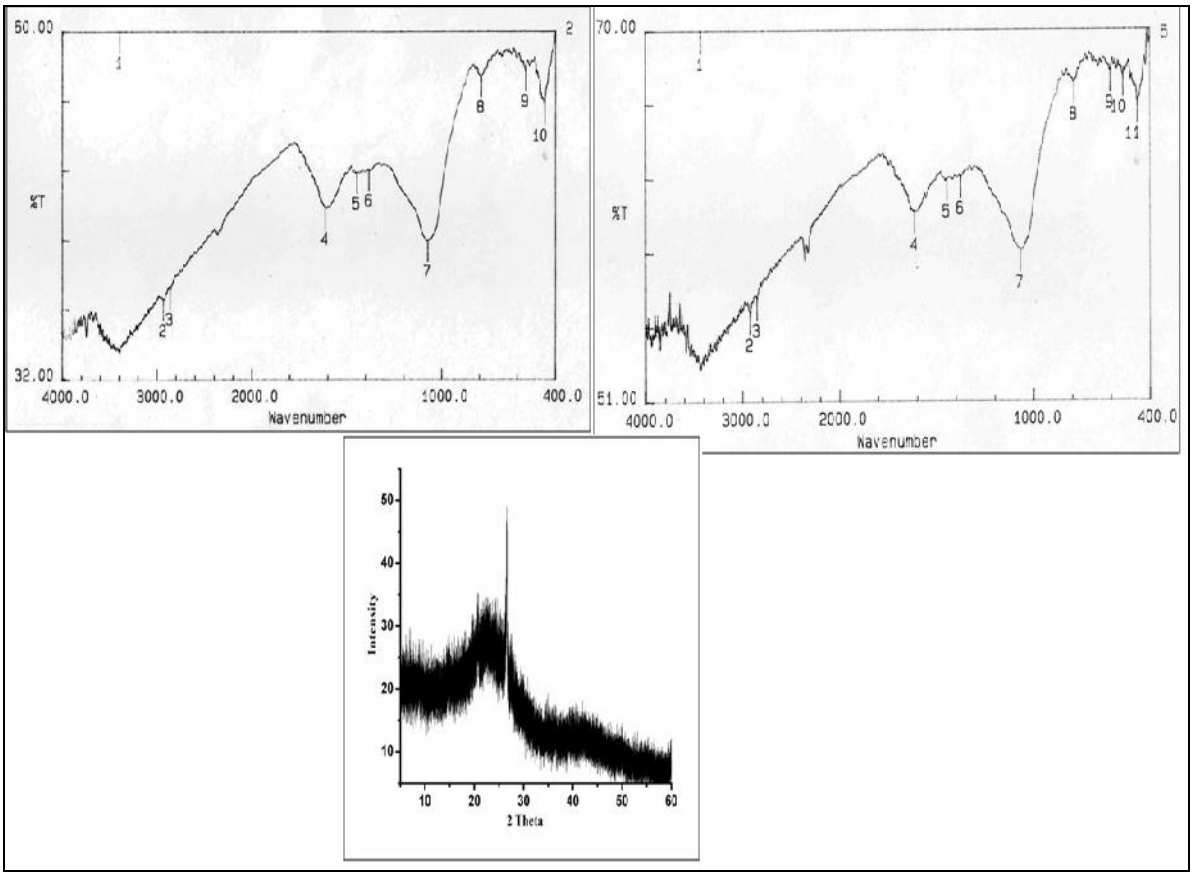

Fig. 2: FTIR Spectrum of LSSC before and after treatment; XRD graph (below)

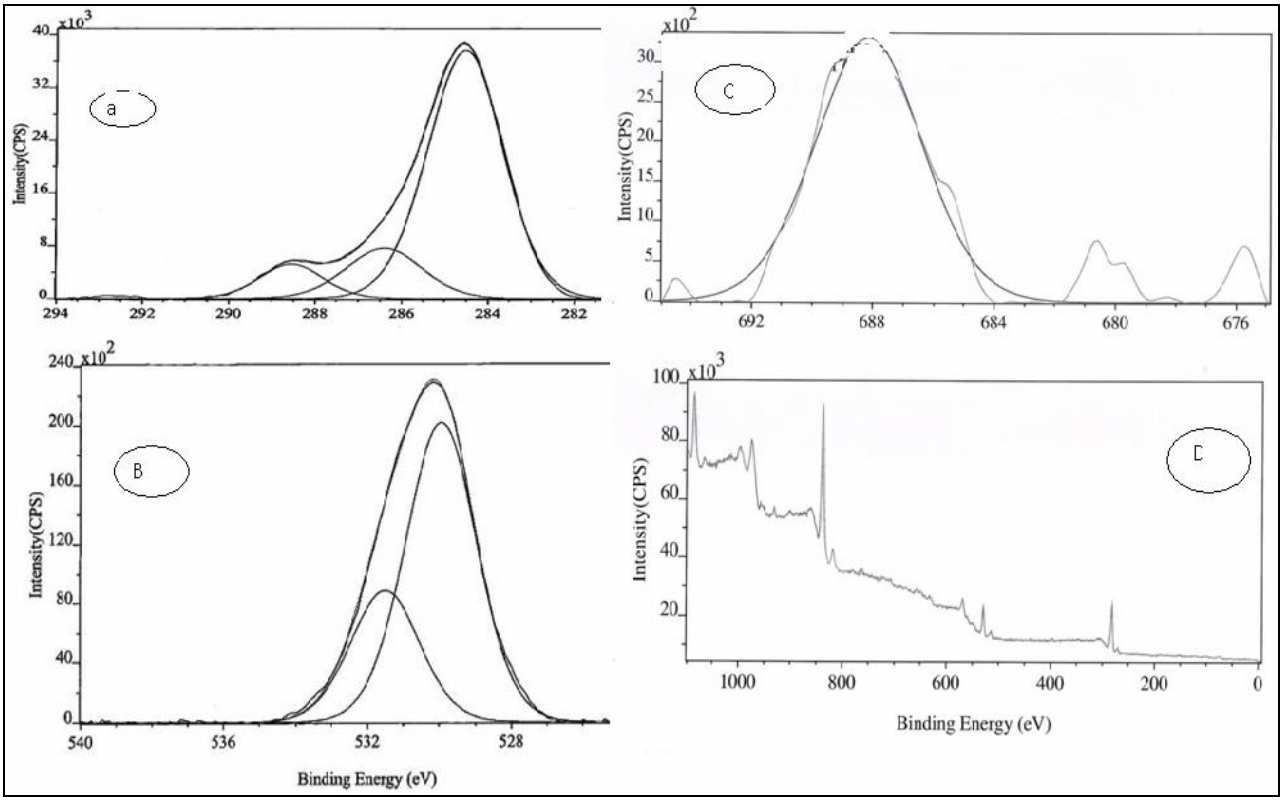

Fig. 3: XPS analysis of LSSC (after defluoridation) a) C1s spectra, b) O1s Spectra c) F1s Spectra, and d) XPS survey scan of LSSC

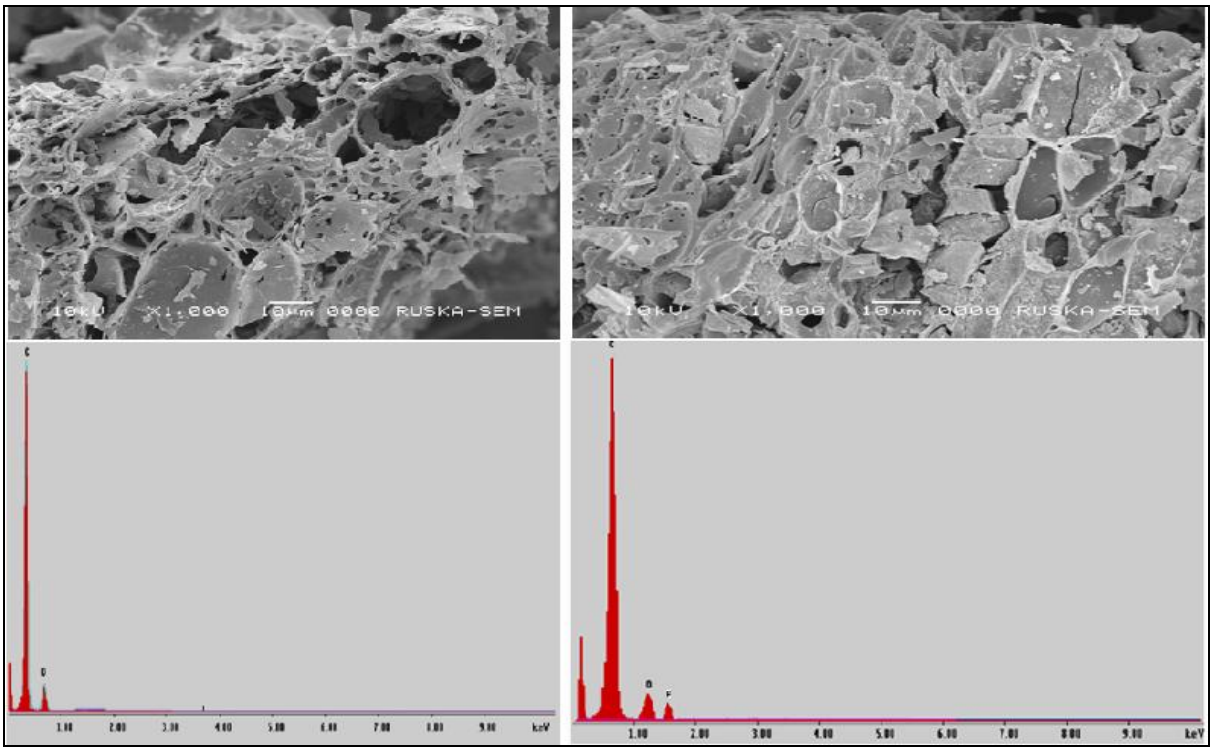

Fig. 4: SEM (above) EDX spectra of LSSC Before (left) and after (right) treatment.

Boehm titration[28-29]: The surface functional groups of oxygen were determined according to Boehm titration. One gram of carbon sample was placed in 50 ml of the solution containing 0.1 mol/L of sodium hydroxide, 0.05 mol/L sodium carbonate, and 0.1 mol/L of sodium bicarbonate. The bottles were sealed, shaken for 24 h, and the mixture was filtered subsequently. The excess base was titrated with 0.1M HCl solution. The value of acidic sites was determined under the assumptions that NaOH neutralizes carboxylic, lactonic and phenolic groups; that Na_2CO_3 neutralizes carboxylic and lactonic groups; and that $NaHCO_3$ neutralizes only carboxylic groups. 0.1 mol/L NaOH solution was titrated with 0.1 mol/L HCl and it was taken as blank value. The mass of surface acid functional groups (SAFG) was calculated by following equation

$$mass\ of\ SAFG = \frac{0.1 \times f \times (Tb - T) \times \frac{50}{20}}{w\left(m.\frac{mol}{g}\right)}$$

where Tb (ml) is the titration mass of 0.1 mol/L HCl for the blank experiment, T (ml) the mass of 0.1 mol/L HCl consumed in different filtrated solution, w(g) the mass of activated carbon i,e. 1 g in this experiment, and f is the constant.

X-ray Diffraction (XRD) Analysis: The XRD analysis on the prepared samples was made using a SCINTAG X'TRA AA85516 (Thermo ARL) X-ray diffractometer equipped with a Peltier cooled Si solid detector. Monochromatized Cu KR1 (0.150 -54 nm) was used as the radiation. Diffraction patterns were collected at 45 kV–40 mA, at 0.02°C step and count time of 0.400 sec over a range of 10.00–80.0 (2θ), at a step scan rate of 3.00 min^{-1}.

Fluoride ion analysis: Fluoride ion concentrations were measured using a specific fluoride combination electrode (ISE 25) connected to an Orion 3-Star ion meter after the total ionic strength adjustment. A total ionic strength adjustment buffer was used to adjust pH during the measurement. The percentage removal of F^- ion and amount adsorbed per gram of sorbent (in mg/g) were calculated using the following relationships:

Percentage removal $(\%R) = \frac{C_i - C_e}{C_i} \times 100$

Amount adsorbed $q_e = \frac{(C_0 - C_e)}{W}$

where Ci and Ce are the initial and final concentrations (mg/L) of F^- ion respectively and 'm' is the mass of carbon (mg/L). Blanks without F^- ions were used for each series of experiments as controllers. The average values of duplicate runs were obtained and analyzed. Error in data was: ±1– 2% for percentage removal, ± 0.005–0.01 mg/g for amount adsorbed.

Results And Discussion

Adsorbent characterization: The results of BET surface area studies are presented in Table 1: b. It is observed from the results that there is reduction in surface area, pore size and pore volume for LSSC before and after sorption of fluoride. The surface area is reduced from 198.502 m^2/g to 149.77 m^2/g, the pore size from 20.283 to 15.274 Å and pore volume from 1.088 to 0.715 cc/g. This reduction may be due to the sorption of Fluoride ions on the surface.

From the studies of elemental analysis, it was observed that a small amount of nitrogen (0.52%) was introduced in to the adsorbent due to nitric acid oxidation. Further a marked difference observed in carbon and hydrogen contents, reveals the ability of modified samples (Table 1a). The high-resolution scans of XPS were performed over the 280– 294, 395–407, 527–540eV 680-700eV ranges (C1s, O1s and F1s spectra, Fig. 2 respectively) for samples before and after fluoride adsorption. XPS spectra of the C1s and O1s regions showed that carbon-based surface oxide groups were present in the sample. The range of the main peak position (BE) and the relative peak area (r.p.a.) for separate peaks were estimated and were presented in Table 1c.

Table 1a: Surface analytical studies of LSSC

Elemental analysis (%)		**FTIR analysis**		
C	80	Peak no.	LSSC-B	LSSC-A
H	2.02	1	3435.53 (43.0)	3395.02 (34.2)
N	0.52	2	2916.63 (47.8)	2937.06(38.4)
S	0.2	3	1691.72(56.0)	2860.69(39.3)
Others by difference	17.26	4	1616.49(54.3)	1614.56(45.8
Surface functional groups (%) (Boehm titration)		5	1425.52 (57.2)	1446.74(48.6)
Carboxyl	0.96	6	1315.57(57.7)	1383.09(48.9)
Lactonic	Nil	7	1105.31(59.2)	1074.45(43.2)
Phenolic	1.12	8	1022.36 (60.5)	790.89(56.4)
Carbonyl	1.26	9	831.39 (64.3)	555.55(56.9)
Total basic groups,	6.82	10	763.88(64.6)	457.17(54.1)

*LSSC-B (Before), LSSC-A (After)

Table 1b: Surface analytical studies of LSSC

XPS analysis			
Name	Energy	Area	%
C 1s	284.582	21172.6	56.5
C 1s	286.417	12315.8	32.9
C 1s	287.964	2679.5	7.1
C 1s	289.403	1318.9	3.5
O 1s	529.718	40649.7	62.4
O 1s	531.434	24453.3	37.6
F 1s	688.587	17661.1	100
BET Surface area	Before	After	
Surface area (m^2/g)	198.502	149.77	
Pore Volume (cc/g)	1.088	0.715	
Pore size (Å)	20.283	15.274	

Table 1c: Elemental composition from EDX before and after defluoridation

	Before		After	
Element	Wt %	At %	Wt %	At %
C K	87.4	87.6	87.2	87.4
O K	12.6	12.4	11.4	11.3
F K	nil	Nil	1.4	1.3
Total	100	100	100	100

Deconvolution of the C1s spectra (Fig. 2) yielded four peaks with different binding energies (BE) representing graphitic carbon (284.584 eV), carbon present in structural hydroxy-and ether-like groups (286.417 eV), carbonyl or quinone groups (287.964 eV), carboxyl or ester (anhydride) groups (289.403 eV). These assignments agreed very well with the extensive XPS studies made on the commercially available carbons used as catalyst supports [30-31] The O1s spectra (Fig. 3) for the carbon samples displayed two main peaks corresponding to the C=O (529.718 eV) and C–O (531.434 eV) moieties in different surface oxygen-containing functional groups[32-33]. After the defluoridation of standard fluoride solution with LSSC, the representative high-resolution narrow scan for F 1s was shown in Fig. 3. The main peak at nearly 688.6 eV indicated the adsorption of fluoride on activated carbon. In the present investigation, the peak in XPS spectra for fluoride was not observed before defluoridation with LSSC. So, it could be concluded from the obtained results that the sample is rich in carbon and Oxygen than any other elements and after sorption, some F^- ions are bounded to the surface of the activated carbon. Details of phase structure and the process of graphitization of carbon material were obtained from XRD studies. The XRD pattern of carbon material was shown in Fig. 2. Above a 2 value of 27°, several sharp and intense diffraction peaks were observed in the XRD profile of LSSC and they were a result of silica and other typical mineral matters presented in the plant tissues which remained intimately bound with carbon material.

Fourier transform infrared (FT-IR) spectrum for the active carbon before and after absorption had been registered and was presented in the Fig.2. On inspection of the characteristic peaks, it was evident that the prominent sharp and intense band centered around 1691 cm^{-1} could be attributed to the carbonyl (C=O) stretching vibration of quinine[33-34]. The Quinine type carbonyl groups would have been generated on the surface of the active carbon due to the oxidation caused by treating the sorbent with Conc. HNO_3. Literature reports that such carbonyl functional groups are known to be pronounced in the case of oxidized carbon materials rather than the original parent carbon material [34]. Further, a broad and intense band having the centre at 3435 $cm^{-1}$was observed in the range of 3200 – 3600 cm^{-1} and it could be assigned to the O-H stretching vibration of surface hydroxyl groups of sorbent and also due to the sorbed water. The asymmetry of this band (a shoulder at lower wave number, 3395cm^{-1}) indicates the presence of strong hydrogen bonding interactions (after defluoridation, may be 'O-H-F' type)[33-34]. The peaks at 2916 and 2937 cm^{-1} could be due to aliphatic asymmetric C-H stretching vibration of methylene groups[33, 35] and 1425 and 1446 cm^{-1} peaks could be due to in plane bending vibration of C-H of methylene group[35]. C-O stretching in phenols, alcohols, acids, ethers and esters were evident from the peaks in the range 1000 - 1300cm^{-1} [34-35].

The results of Boehm titration were presented in Table 1a. The Boehm titration results indicated the absence of lactonic groups and this fact was also confirmed by FT IR spectra. Carboxylic acid groups (0.96%), phenolic (1.12%) and carbonyl (1.26%) groups were identified and these were confirmed by XPS and FTIR studies.

The adsorbent sample made in this study was characterized before and after defluoridation by scanning electron microscopy (Fig. 4). Samples were platinum coated prior to SEM observations. SEM spectra showed that the adsorbent sample had an irregular and porous surface, which resulted in high surface areas.

Elemental analysis was done by EDX spectra and the obtained spectra were presented in Fig 4 and the data was presented in Table 1c. The absence of fluoride peak before treatment but its presence after sorption experiments indicates that the Fluoride was onto the LSSC surface.

Effect of pH and surface loadings: The effect of pH on fluoride adsorption was examined at the F^- ion concentration of 5 mg/L and sorbent concentration of 4.0 g/L. The results are presented in Fig. 5. It is observed that more than 65% adsorption is noted in the pH range 5.0 to 7.0 with maximum adsorption peak at pH: 6.8. Further, adsorption peak in the pH rage: 5-8, is found to be broader in lower surface loading conditions while

it is narrower under higher surface loading conditions.

The observed data may be accounted that protonated surface sites are normally responsible for anion adsorption. So, acidic conditions favor the F^- adsorption on to LSSC surface. However, according to fluoride speciation, hydrofluoride (HF) is predominant in pH conditions less than 3.0 [36] and so less sorption is observed at pH values less than 3.Thus, optimum pH range of adsorption is found to be 6.0 to 7.0 wherein more than 85% of removal of fluoride is observed.

Effect of initial adsorbate concentration: The effect of initial concentration of fluoride on the % removal of fluoride by LSSC adsorbent has been studied by varying the initial concentration of fluoride between 1.50 – 15.0 mg/L at a fixed concentration of adsorbent: 4.0 g/L, time of equilibration: 40 minutes, and temperature:30 ± 1^oC. It is found that the percentage removal of fluoride decreases with the increase in the initial concentration of the fluoride (**Fig. 5).** This may be due to the lack of sufficient number of available active sites on the adsorbent surface in contrast to the relatively large number of active sites required for the adsorption of high initial concentrations of fluoride ions. The results indicate that when the concentration of fluoride increases from 1.5 to 14.5 mg/L, percent removal of fluoride decreases from 100.0 to 43.20. Further, it is noted that the amount of fluoride adsorbed on the LSSC adsorbent, increases with the increase in the initial concentration of the fluoride. It is found that the fluoride adsorption on the fixed amount of adsorbent is changed from 0.375 to 3.040 mg/g as the concentration of fluoride increases from 1.5 to 15.0 mg/L.

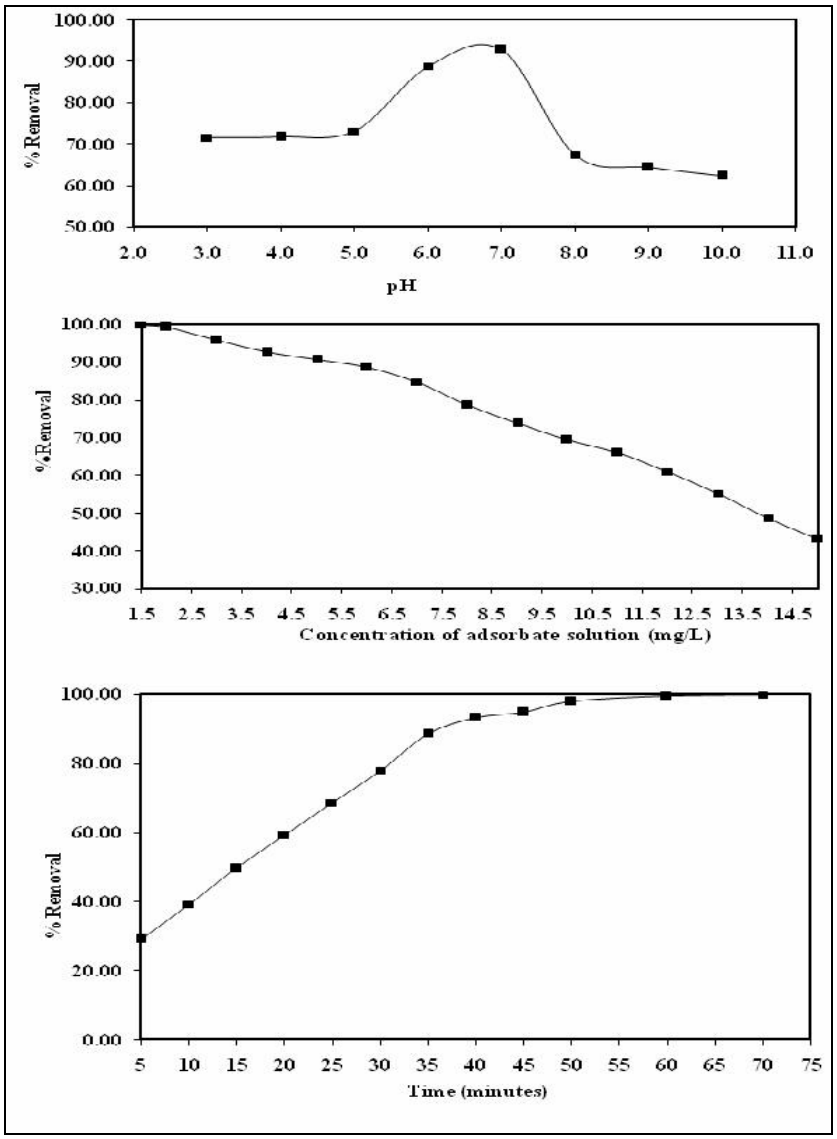

Fig. 5: Effect of pH, Concentration of fluoride ion and time on adsorption of fluoride (from clock wise direction)

Adsorption isotherms: The adsorption isotherm is the most extensively employed method for representing the equilibrium states of an adsorption system. The purpose of an adsorption isotherm is to relate the adsorbate concentration in the bulk solution to the amount adsorbed at the solid/solution interface. The analysis of isotherm data is important in developing an equation which accurately represents the results and which can be used for design purposes. The Langmuir and Freundlich adsorption isotherm equations[37] are in common use for describing adsorption isotherms at a constant temperature for water and wastewater treatment applications.

Linear form of Freundlich isotherm equation is: $\log(q_e) = \log K_f + \left(\frac{1}{n}\right)\log(C_e)$

where K_f and 1/n are the Freundlich constants.

Linearized Langmuir equation is: $C_e/q_e = 1/k_L + a_L/k_L\, C_e$ and its important features can be defined by the dimensionless constant separation factor R_L[38] which is expressed as:

$R_L = 1/(1+bC_i)$,

Where C_i is the initial F^- ion concentration, q_e (mg/g) is the amount of F^- ions adsorbed per unit weight of the adsorbent (mg/g), a_l and b are the Langmuir constants related to capacity and energy of adsorption, respectively.

In the present work, plots of log (C_e) Vs log (q_e) at different F^- ion concentrations are found to be linear as shown in the Fig. 6 and confirm the applicability of Freundlich isotherm model. When Ce/qe is plotted against Ce, a straight line with slope 1/ba is obtained which shows that the adsorption follows the Langmuir isotherm as shown in Fig. 6. The Langmuir constants 'b' and 'a' are calculated from the slope and intercept with Y-axis. The values of the Freundlich and Langmuir adsorption constants together with the correlation coefficients are presented in **Table 2.** The observed linear relationships are statistically significant as evidenced from the correlation coefficients (r-values) close to unity, which indicates the applicability of these two adsorption isotherms and the monolayer coverage of F^- ion species on the carbon surface. The magnitudes of K_f and 1/n are calculated from the intercept and slope of the plots.

Table.2: Adsorption isotherm data

S.No.	Isotherm name	Parameter	Value
1	Freundlich	K_F	0.2380
		1/n	0.4990
		'r'	0.9924
		R^2	0.9850
2	Langmuir	*a*	0.3180
		b	0.0.088
		'r'	0.9930
		R^2	0.9860
		R_L	0.2084

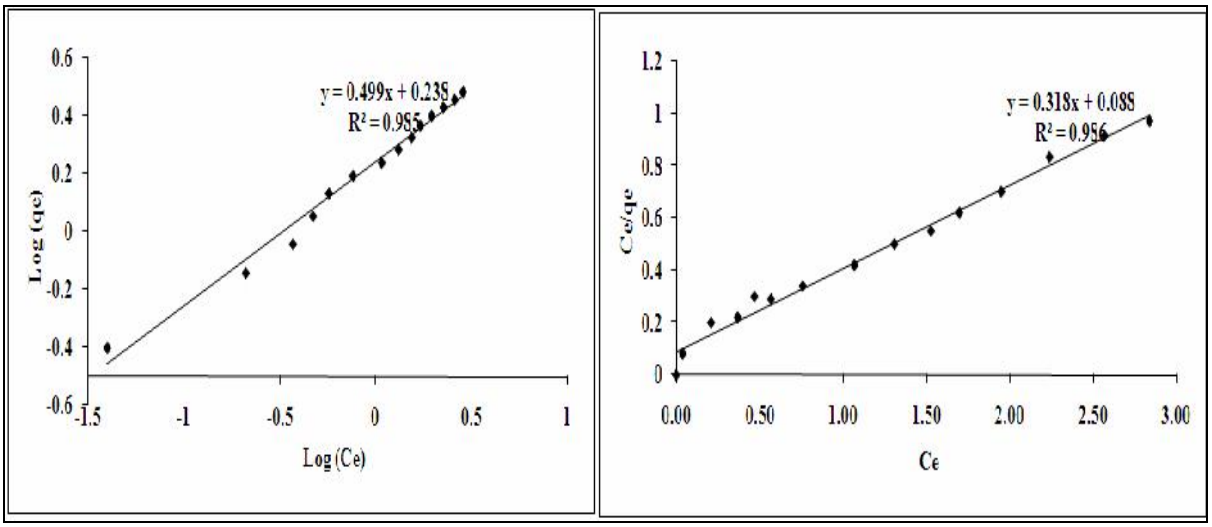

Fig. 6: Freundlich isotherm (Left), Langmuir isotherm (Right)

According to Hall et al [38] the separation factor R_L indicates the isotherm's shape and the nature of the adsorption process as unfavorable ($R_L > 1$), linear ($R_L = 1$), favorable ($0 < R_L < 1$) and irreversible ($R_L = 0$). In the present study, the computed values of R_L (Table 1) are found to be fraction in the range of 0-1, indicating that the adsorption process is favorable for the adsorbent in the removal of F^- ions.

Effect of agitation time: In the adsorption system, agitation time plays a vital role irrespective of the other experimental parameters that affect the adsorption kinetics. So, the % of removal of fluoride was studied by varying the time of equilibration (5-70 minutes) at fixed optimum conditions of pH, sorbent dosage and initial concentration of fluoride. The results were presents in Fig. 5. It can be noted that the percentage of fluoride removal is increasing with time and attained almost an equilibrium condition in about 40 minutes at which, the rate of adsorption of solute is equal to the rate of desorption. The decrease in the removal of rate of fluoride, particularly towards the end indicates a possible monolayer of fluoride on the outer interface of the activated carbon and pore (intra-particle) diffusion on to the inner surface of the adsorbent particles through the film due to continuous agitation maintained during the experiments [39]. Further, the removal of fluoride by the adsorbent is rapid at the initial period but becomes slow and almost stagnates with the increase in the contact time. The relative increase in the removal of fluoride is substantially low after 40 minutes of contact time by the adsorbents, which is fixed as the optimum contact time. This indicates that the rate of removal of fluoride is higher in the initial stage due to the availability of adequate surface area of the adsorbent. With increase in contact time, the adsorption process decreases and it is attributed to the decrease in the availability of active sites.

Kinetic study of adsorption process: The kinetics of sorption describes the solute uptake rate, which in turn governs the residence time of sorption reaction. It is one of the important characteristics in defining the efficiency of sorption [40]. In the present study, the kinetics of F^- ion removal was carried out to understand the behavior of prepared low cost carbon adsorbent and the corresponding data was given in Table 3.

The pseudo first-order equation [41] is:

$$\log_{10}(q_e - q_t) = \log_{10} q_e - K_1 t$$

It was found in this work that the values of log (q_e - q_t) were linearly correlated with t. From, the linear plot of log (q_e - q_t) vs. t , k_1 and q_e could be determined from the slope and intercept of the plot (Fig.7), respectively.

First order kinetics **(**Lagergren) [41,42]: In order to find out whether the adsorption process followed first order kinetics, the following generalized first order kinetic equation proposed by M. R. Unnithan[43] was employed. The linearized form of first order equation is represented as follows:

$$\log_{10}(q_e - q_t) = \log_{10} q_e - \frac{K_{ads}\, t}{2.303}$$

Where q_t is the amount of F^- ion adsorbed (in mg/g) at various times, t, q_{max} is the maximum adsorption capacity and K_1 is the first order rate constant for the adsorption process (min^{-1}). In the present work, linear correlations of $1/q_t$ Vs 1/t are found (Fig. 7) and the results are given in Table 3

Pseudo-second-order kinetic model: The pseudo second-order adsorption kinetic rate equation [44] is expressed as: $\frac{t}{q_t} = \frac{1}{h} + \frac{1}{q_e}(t)$

and it is used in this work.

The plot of (t/qt) and't' for LSSC, gave a linear relationship and qe and k_2 were determined from the slope and intercept of the plot (Fig. 7), respectively.

Second order rate equation [45]: The following integrated rate expression was used to calculate the second order' rate constants: $\frac{1}{C_e} - \frac{1}{C_i} = K_{ad} t$

where Ci is the initial concentration of the F^- ion solution, and Ce is the concentration at time t.

From the slopes of the linear plot (t Vs $\frac{1}{C_e} - \frac{1}{C_i}$) as depicted in the Fig.7, the adsorption coefficient (k_{ad}) value for LSSC was calculated.

Intraparticle diffusion model [45]: The mathematical expression for the intraparticle diffusion model is $qe \approx kp\, t^{0.5}$ where kp (mg/g $min^{-0.5}$) is defined as the intraparticle diffusion rate constant and is related to the intraparticle diffusivity in the following way,

$$k_p = \frac{6 q_e}{R}\sqrt{\frac{D}{\pi}}$$

where R (cm) is the particle radius and qe (mg/g) is the solid phase concentration at equilibrium. The plot of the average particle loading, qe (mg/g), versus the square root of time, $t^{0.5}$ (Fig. 8), would yield a straight line passing through the origin, if the adsorption process obeys the intraparticle diffusion model. The slope of the straight line equals to k_p, the intraparticle diffusion rate constant.

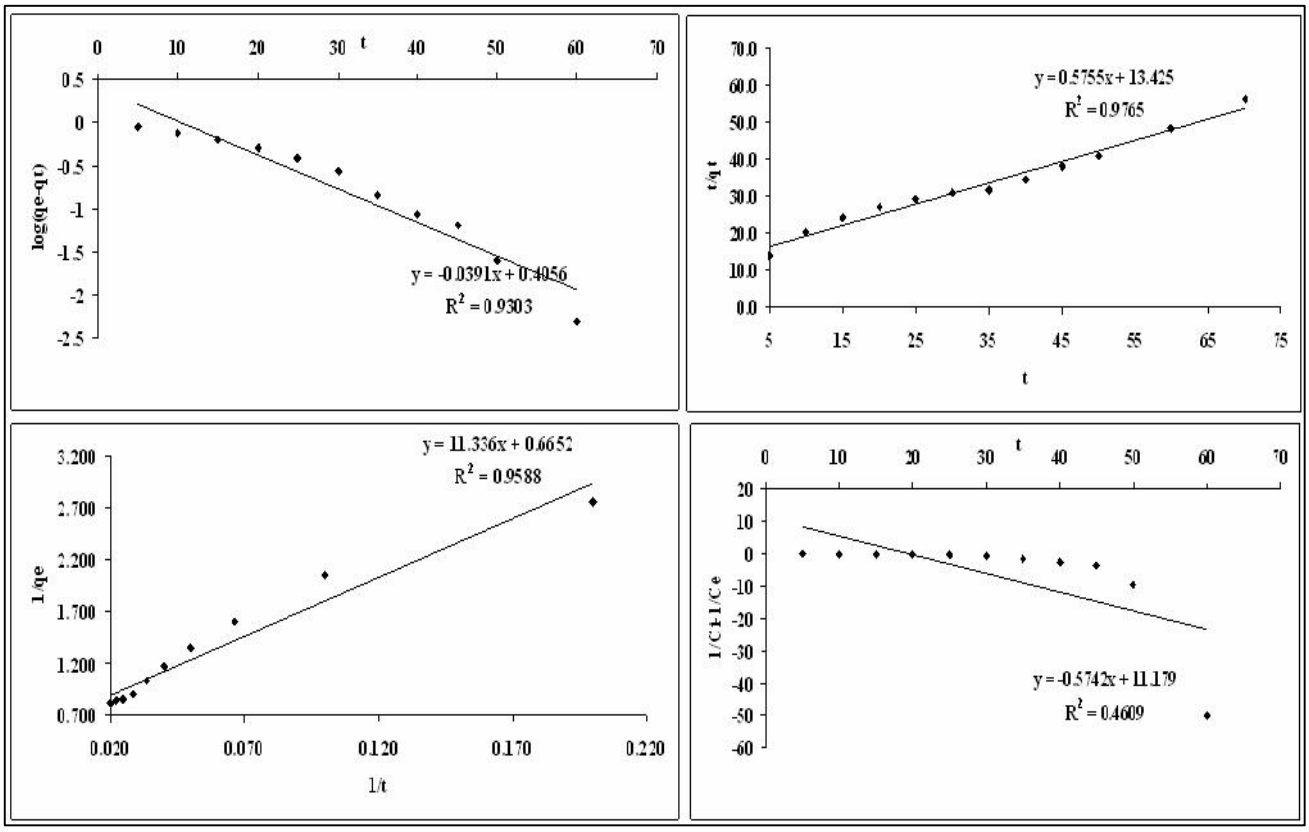

Fig. 7: Kinetics of adsoprtion studies from clock wise direction Pseudo first-order, Pseudo second-order, First order, and Second order kinetics

Pore diffusion model (Bangham's equation)[45]: In order to confirm further the occurrence of intraparticle diffusion, the Bangham equation was applied to the sorption data in the following form:

$$\text{Log Log}\left(\frac{Q_o}{Q_o - Q_t W}\right) = \log\left[\frac{k_o w}{2.303\,V}\right] + \alpha \log(t)$$

where Qo is the initial concentration (mg/g) of F^- ion in the solution, V is the volume of sorbate solution (ml), W is the weight (g) of sorbent, Qt is the amount of adsorbate sorbed (g/g) at time t, while α and k_o are constants. Using the kinetic data for LSSC uptake at room temperature, fair linear plot was obtained between log (log Q_o/Q_o-Qt) and log (t) (Fig. 8) which confirmed the validity of Bangham equation. The values of α and k_o, are calculated from the slope and intercept of the linear plot.

Table .3: Adsorption kinetic parametres

Pseudo first order kinetics		*Second order kinetics*	
q_e	0.0391	q_e	11.17
K1	0.4056	K_{ad}	0.5742
R	0.9645	R	0.6788
R^2	0.9303	R^2	0.4609
First order kinetics		*Intraparticle diffusion model*	
q_{max}	11.336	Qe	0.025
K1	0.6652	Kip	0.1646
R	0.9791	R	0.9718
R^2	0.9588	R^2	0.9445
Pseudo-second-order kinetics		*Pore diffusion model*	
q_e	0.5755	K_o	1.785
K_2	13.425		1.141
R	0.9881	R	0.9699
R^2	0.9765	R^2	0.9408

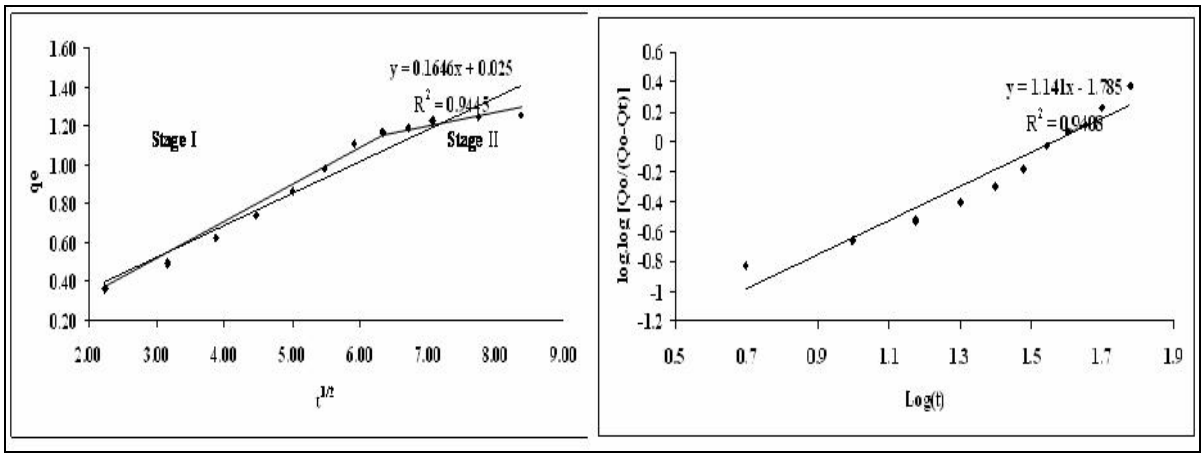

Fig. 8: Intra particle diffusion model (Left), Pore diffusion model (Right)

Comparison of the applicability of different kinetic models: In order to test the applicability of the five different kinetic models, namely the Pseudo first order, First-order, pseudo-second-order, second order, and the intraparticle diffusion model, the experimental data was correlated with the linear forms of the five models respectively. The derived rate constants together with the correlation coefficient for the adsorption system have been listed in Tables 3 and it displays the best-fitting results by the pseudo-second-order rate equation. Several conclusions can be drawn from Tables 3.

Among the five kinetic models, the pseudo-second-order equation generates the best fit to the experimental data of the present investigated adsorption system. The correlation coefficient obtained is greater than 0.98 and this indicates that the pseudo-second-order equation is potentially a generalized kinetic model for the adsorption study.

However, it seems that there is no general "second best" model to describe the sorption system. The other models fitness is of the order of: First-order rate equation (R^2=0.9588) followed by the intraparticle diffusion model (Bhangam model) (R^2 = 0.9408), followed by Pseudo-First-order (R^2 = 0.9303), and lastly the second-order kinetic model (R^2 = 0.4609). It is worth noting that the low correlation coefficients shown in **Table 3** do not necessarily mean that the intraparticle diffusion process is not the rate-controlling step. It is a mere indication that the intraparticle diffusion model does not apply to the present investigating adsorption system. This may be due to the following two reasons: first, the intraparticle diffusion model assumes infinite solution volume control, which implies that there is no change in solution concentration during the approach to equilibrium. This is only achieved when the product of the solution volume and solution concentration greatly exceeds the product of the adsorbent mass and the equilibrium sorption capacity of the adsorbent. However, this is not the case for the present investigated adsorption system. Second, the intraparticle diffusion model is derived assuming a constant diffusivity.

Effect of major anions: Natural water may contain many anions that compete with fluoride for adsorption. In this study, effects of HCO_3^-, SO_4^{2-}, $H_2PO_4^-$and Cl- were examined at pH 6.9. The initial concentration of fluoride was 5.0 mg/L in all experiments, whereas concentrations of other anions were varied from 10 to 300 mg/L. The results show that the fluoride adsorption ratio is decreased from 67% to 40% when the P concentration (in the form of $H_2PO_4^-$) is increased from 0 to 300 mg/L. $H_2PO_4^-$ is adsorbed on LSSC surface as an inner-sphere complex via ion exchange mechanism and LM He et al [46] suggested H^+ ion is replaced from functional groups of the surface: -OH or H_2O. Fluoride adsorption also was decreased substantially when bicarbonate was present in the system. Bicarbonate is a pH buffering agent and its increasing presence in solution buffers the system pH and thereby diminishes the affinity of the active sites of LSSC for fluoride and this result in the reduction of the uptake of Fluoride [47]. Cl^- had less impact on fluoride adsorption, as compared to other anions tested. Previous research indicated that Cl^- formed outer-sphere surface complexes, while SO_4^{2-} formed both outer-sphere and inner-sphere surface complexes [48]. Therefore, the expected impact of Cl^- on Fluoride adsorption is less significant than that of SO_4^{2-}. Overall, the impact of major anions on Fluoride adsorption followed the order: $H_2PO_4^-$

$>HCO_3^-> SO_4^{2-}$, reflecting the relative affinity of these anions for LSSC.

Cost analysis: The relative cost of the material used in the present study is very much lower than that of commercial activated carbons. The Lagenaria siceraria fruits are available abundantly throughout the year and of low cost, and after considering expenses like transport, chemicals, electrical energy and processing cost, the cost of the material would be approximately US $25/ton. This cost can be further brought down after successful regeneration of the used LSSC. The cost of the activated carbon (CAC) used for water treatment in our country is around US $300/ton.[49]

Conclusions

Fluoride adsorption onto LSSC obeys a Pseudo-second-order rate law. Results also indicate that the fluoride adsorption reaches maximum in the pH range of 6.5-7.0, and then decreases with further increasing of pH. At the same pH, the fluoride adsorption follows the Freundlich isotherm, indicating that the LSSC surface is highly heterogeneous. XPS, FTIR, and SEM-EDX characterization show evidence for inner-sphere complexation. In addition, a larger population of surface hydroxyl groups accompanied fluoride adsorption along with increased hydrogen bonding present on the LSSC surface, indicative of an H···F interactions. Major co-existing anions also affect Fluoride adsorption according to their affinity on the LSSC surface.

References

1. Medikondu Kishore and Hanumantharao, Y., Validation of defluoridation method with “acacia arabica” plant byproduct through 2^n factorial experimentation-a statistical approach. Int.J.Appl.Biol.Pharm.Tech, 2010, 1 (3), 1230-1235.
2. Jamode, A.V., Sapkal, V.S., Jamode V.S., and Deshmukh, S.K., Adsorption kinetics of defluoridation using low-cost adsorbents, Adsorption Sci. Technol., 2004, 22, 65–73.
3. Cengeloglu, Y., Esengul, K., and Ersoz, M., Removal of fluoride from aqueous solution by using bauxite wastes. Sep & Pur Tech. 2002, 28, 81 – 86.
4. WHO, Guidelines for drinking water quality, Health criteria and other supporting information. Geneva, Switzerland, 1984, Vol. 2
5. Yadav, A.K., Kaushik, C.P., Haritash A.K., Kansal A., and Neetu R., Defluoridation of groundwater using brick powder as an adsorbent, J. Hazard. Mater, 2006, 128(19), 289–293
6. Nawlakhe, W.G., Kulkarni D.N., Pathak B.N., and Bulusu K.R., Defluoridation of water by Nalgonda technique. Ind. J. Environ. Health., 1975, 17, 26–65.
7. Mjengera, H., and Mkongo G., Appropriate defluoridation technology for use in fluorotic areas in Tanzania, Phys. Chem. Earth, 2003, 28,1097–1104.
8. Lhassani, A., Rumeau M., Benjelloun D., and Pontie M., Selective demineralization of water by nanofiltration application to the defluoridation of brackish water, Water Res. 2001, 35, 3260–3264.
9. Feng Shen, X., Chen P.G., and Guohua C., Electrochemical removal of fluoride ions from industrial wastewater, Chem. Eng. Sci. 2003, 58,987–993.
10. Chubar, N.I., Samanidou V.F., Kouts, V.S., Gallios G.G., Kanibolotsky V.A., Strelko V.V. , and Zhuravlev I.Z., Adsorption of fluoride, chloride, bromide and bromate ions on a novel ion exchanger, J. Colloid Interface Sci. 2005, 291,67–74.
11. Tripathy, S.S., Jean-Luc Bersillon, and Krishna Gopal, Removal of fluoride from drinking water by adsorption onto alum-impregnated activated alumina, Sep. Purif. Technol. 2006, 50,310–317.
12. Sathish, R.S., Raju N.S.R., Raju G.S., Rao G.N., Kumar K.A., and Janardhana C., Equilibrium and kinetics studies for fluoride adsorption from water on zirconium impregnated coconut shell carbon, Sep. Sci. Technol. 2007, 42,769–788.
13. Somasekhara rao, K., Kishore M., and Vani, K.N.K., Water pollution and defluoridation of Vemulapalli mandal drinking water with prepared carbons. Journal of Chemical and Environmental Research, 2007,16 (1&2), 232-238

14. Somasekhara rao, K., Kishore M., and Sarada, D., Water Quality status and Defluoridation studies of Damarlacherla Mandal, Nalgonda District, A.P) Using activated Mango shell carbon. Chem.Environ.Res. 2006., 15 (1&2),164-167
15. Seethapathirao,R., Defluoridation water using sulphated coconut shell carbon, Indian J. Environ. Health. 1964, 64, 11-12.
16. Alagumuthu, G., and Rajan, M. Equilibrium and kinetics of adsorption of fluoride onto zirconium impregnated cashew nut shell carbon, J.Chem. Eng. 2010, 158, 451–457.
17. Alagumuthu, G., and Rajan, M. Kinetic and equilibrium studies on fluoride removal by zirconium (IV) – impregnated ground nutshell carbon, Hem. Ind. 2010, 64 (4), 295–304.
18. Hanumantharao, Y., Kishore M., and Ravindhranath, K., Preparation and development of adsorbent carbon from Acacia farnesiana for defluoridation. International Journal of Plant, Animal and Environmental Sciences, 2011, 1(3), 209-223
19. Somasekhara rao, K., Prasad N.V.V.S., and Kishore M., Physico chemical analysis of A.Kondur revenue sub division and defluoridation studies with activated carbon. Ind.J.Env.Prot, 2005, 25(9),824-828
20. Dahiya, V., and Amarjeet Kaur., Studies on removal of fluoride by coconut coir pith carbon. Ind.J.Env.Prot. 1999,19(11),811-814
21. Uday Simha, L., Panigrahy R.K., and Ramakrishna, S.V., Prelimanary studies on fluoride adsorption by water hycinth. Ind.J.Env.Prot. 2002, 22(5), 506-511.
22. Rama chandra murthy, T., Fluoride estimation in potable water in Tiruchurapalli rock fort area Dental fluorosis survey and defluoridation with Emblica phyllanthus. Ind.J.Env.Prot. 2003, 23 (3) 317-320.5
23. Karthikeyan, G., and Ilango, S.S., Fluoride sorption using Morringa based activated carbon. Iran.J.Environ.Health.Sci.Eng., 2007, 4(1), 21-28
24. Radovic, L.R., and Rodriguez-Reinoso, F., In Chemistry and Physics of Carbon thower, P. A. Ed Marcel Dekker, New York, 1997,25, 243
25. Venter, J.J., and Vannice, M.A., Applicability of “drifts” for the characterization of carbon-supported metal catalysts and carbon surfaces. Carbon, 26, 889.
26. Meldrum, B.J., and C. H. Rochester, 1990. In situ infrared study of the surface oxidation of. activated carbon in oxygen and carbon dioxide J. Chem. Soc.Faraday Trans, 1988, 86,2997
27. Abdel-Nasser, A., El-Hendawy, Samra, S.E., and Girgis, B.S., Adsorption characteristics of activated carbons obtained from corncobs, Colloids and Surfaces A, Physicochem. Eng. Aspects, 2001,180, 209–221
28. Kadirvelu, K., Faur-Brasquet, C. and Le Cloirec, P., Removal of Cu (II) Pb (II) and Ni(II) onto activated carbon cloth. Langmuir, 2000, 16, 8404–8409
29. Boehm, H.P., Tereczik, B.,and Schanz, K., Proc. Colloque Intern. Adsorption Interfaces gaz/solide, Aix-en-Provence, Elsevier, 1982, 395,
30. Albers, P., Deller K., Despeyroux B.M., and Prescher G., SIMS/XPS investigations on activated carbon catalyst supports. J. Catalysis, 1994,150, 368-375
31. Moreno-Castilla C., Lopez-Ramon M.V., and Carrasco-Marin F., , Changes in surface chemistry of activated carbons by wet oxidation. Carbon, 2000, 38, 1995-2001
32. Biniak, S., Swiatkowski A., Pakula M., and Radovic L.R., Chemistry and physics of carbon, New York, Marcel Dekker 2001, 27, 125–225
33. Andrzej Swiatkowski, Maciej Pakula, Stanislaw Biniak,Mariusz Walczyk, Influence of the surface chemistry of modified activated carbon on its electrochemical behaviour in the presence of lead(II) ions Carbon2004, 42(15), 3057–3069
34. Ishizaki, C., and Marti I., Surface Oxide Structures on a Commercial Activated *Carbon*. Carbon, 1981, 19, 409
35. Puziy, A.M., Poddubnaya O. I., Martinez – Alonso A., Suarez – Garcia F., and Tascon J. M. D., Synthetic carbons activated with phosphoric acid III. Carbons prepared in air. Carbon, 2003, 41,1181-1191
36. Kannan, N., and Thangadurai Veemaraj, Cadmium (II) ions removal by adsorption onto eucalyptus globules bark, bambusa glaucescens dust and commercial activated carbons. EJEAFChe, 2010, 9 (1), 129-137.
37. Aksu, Z., and Donmez, D. A comparative study on the biosorption HCl treated cracteristics of same yeasts for Ramazol Blue reactive dye. Chemosphere, 2003, 50,1075-1083
38. Hall, K.R., Eagleton L.C., Acrivos A., and Vermevlem T., Pore and solid diffusion kinetics in fixed bed adsorption under constant pattern conditions. Indian. Eng. Chem. Foundation. 1966, 5,212–219

39. Bhargava, D.S., and Killidar D.J., Batch studies of water defluoridation using fish bone char coal .Res. J.WPF. 1991, 63(6), 848-858
40. Hema, M., and Arivoli S., Comparative study on the adsorption kinetics and thermodynamics of dyes onto acid activated low cost carbon. International Journal of Physical Sciences, 2007, 2(1) , 010-017
41. Ho, Y.S., Citiation review of Lagergren kinetic rate equation on adsorption reactions, Scientometrics, 2004, 59, 171–177
42. Sunil Kumar Bajpai, Mukesh Kumar Armo and Mini Namdeo, Removal of CuII From Aqueous Solutions, Acta Chim.Slov. 2009, 56, 254–261
43. Unnithan, M.R., Vinod V.P., and Anirudhan T.S., Ability of iron (III) -loaded carboxylated polyacrylamide-grafted sawdust to remove phosphate ions from aqueous solution and fertilizer industry wastewater, Adsorption kinetics and isotherm studies. J. Appl. Polym.Sci, 2002,84, 2541–2553
44. Yang X. , and Al-Duri B., Kinetic modeling of liquid-phase adsorption of reactive dyes on activated carbon, Journal of Colloid and Interface Science, 2005., 287, 25–34
45. Aharoni, C., Sideman S., and Hoffer. E., Adsorption of phosphate ions by colloid ion-coated alumina, J. Chem. Technol. Biotechnology. 1979, 29, 404-412
46. He, L.M., Zelazny L.W., Baligar V.C., Ritchey K.D., and Martens D.C., Ionic strength effects on sulfate and phosphate adsorption on g-alumina and kaolinite, triplelayer model, Soil Sci. Soc. Am. J. 1997, 61, 784–793
47. Onyango, M.S., Kojima Y., Aoyi O., Bernardo E.C., and Matsuda H. J., Adsorption equilibrium modeling and solution chemistry dependence of fluoride removal from water by trivalent-cation-exchanged zeolite F-9. Colloid Interface Sci. 2004, 279,341–350
48. Tor, A., Cengeloglu Y., Aydin M.E., and Ersoz M. J., Removal of phenol from aqueous phase by using neutralized red mud, Colloid Interface Sci. 2006, 300, 498–503
49. Kadirvelu, K., Karthika, C., Vennilamani, N., and Pattabhi, S., Activated carbon from industrial solid waste as an adsorbent for the removal of Rhodamine-B from aqueous solution, Kinetic and equilibrium studies, Chemosphere, 2005, 60,1009–1017

*****